
REPORT No. 207

**AERODYNAMIC CHARACTERISTICS OF AIRFOILS
AT HIGH SPEEDS**

By L. J. BRIGGS, G. F. HULL, and H. L. DRYDEN

Bureau of Standards



REPORT No. 207

AERODYNAMIC CHARACTERISTICS OF AIRFOILS AT HIGH SPEEDS

By L. J. BRIGGS, G. F. HULL, and H. L. DRYDEN

SUMMARY

This report deals with an experimental investigation of the aerodynamical characteristics of airfoils at high speeds, made at the request and with the financial assistance of the National Advisory Committee for Aeronautics. The investigation was carried out jointly by the Bureau of Standards and the Ordnance Department, United States Army, and was made possible through the courtesy of the Lynn Works of the General Electric Co., where a large centrifugal compressor was made available for the purpose.

Lift, drag, and center of pressure measurements were made on six airfoils of the type used by the Air Service in propeller design, at speeds ranging from 550 to 1,000 feet per second. The results show a definite limit to the speed at which airfoils may efficiently be used to produce lift, the lift coefficient decreasing and the drag coefficient increasing as the speed approaches the speed of sound.

The change in the lift coefficient is large for thick airfoil sections (camber ratio 0.14 to 0.20) and for high angles of attack. The change is not marked for thin sections (camber ratio 0.10) at low angles of attack, for the speed range employed.

At high speeds the center of pressure moves back toward the trailing edge of the airfoil as the speed increases.

The results indicate that the use of tip speeds approaching the speed of sound for propellers of customary design involves a serious loss in efficiency.

INTRODUCTION

This report deals with an investigation of the characteristics of airfoils at high speeds and was made for the purpose of obtaining information for use in the design of propellers. The direct mounting of the propeller on the engine crank shaft avoids the weight and power loss of the speed reduction gear, and possesses other advantages which have made this form of drive very popular. The development of high-speed engines, however, involves the corresponding increase in the tip speeds of propellers mounted on the engine shaft, and it is important to know what performance may be expected from propellers operating at high tip speeds.

There are two published investigations on this subject. Airfoils have been studied up to speeds of about 650 feet per second in the 14-inch wind tunnel of the Army Air Service at McCook Field and the results are given in Report No. 83 of this committee.¹ Direct measurements of the performance of a model air propeller at tip speeds in excess of the speed of sound have been made in England and are described in R. & M. No. 884 of the British Aeronautical Research Committee.² The results given in these two contributions are discussed later under "Comparison with previous work."

The experimental observations here described were made by Dr. L. J. Briggs, Dr. H. L. Dryden, and Mr. W. H. Cottrell, all of the Bureau of Standards, and Lieut. Col. G. F. Hull of the Ordnance Department, United States Army. The computations and curves were made in the aerodynamical physics section of the Bureau of Standards by Dr. H. L. Dryden and Mr. G. C. Hill.

¹ Wind Tunnel Studies in Aerodynamic Phenomena at High Speeds. Part III. F. W. Caldwell and E. N. Fales, Technical Report No. 83, National Advisory Committee for Aeronautics, 1920.

² The Effects of Tip Speed on Airscrew Performance. G. P. Douglas and R. McKinnon Wood. R. & M. No. 884, Aeronautical Research Committee, Great Britain.

APPARATUS AND METHODS

The air stream was supplied by a large turbine-driven 3-stage centrifugal compressor, capable of delivering 50,000 cubic feet or more of free air per minute at gauge pressures up to 15 pounds per square inch. The compressed air delivered by the machine passed through a gate valve in a horizontal pipe to a vertical standpipe 30 inches in diameter and 30 feet high, ending in a cylindrical orifice or nozzle 12.24 inches in diameter. The speed of the free air stream issuing from the nozzle depended upon the gauge pressure and the temperature of the air in the pipe. Air speeds approaching the speed of sound were obtained.

The airfoils tested were members of a series of propeller sections of the form adopted by the engineering division of the Air Service as standard for propeller design. Six airfoils were used, the camber ratios, or ratios of maximum thickness to chord, being 0.10, 0.12, 0.14, 0.16, 0.18, and 0.20, respectively. The chord length was 3 inches and the span 17.2 inches so that the airfoils extended entirely across the jet, and there were no ends exposed to the stream as in ordinary wind-tunnel practice. The dimensions of the airfoils as measured by the gauge section of the Bureau of Standards are given in Table I. The models were of steel and were constructed by Mr. W. H. Nichols at Waltham, Mass. The extreme ends of the airfoils were left in the form of rectangular blocks to fit in the holding grooves of the balance fork described below. The blocks were so located with respect to the airfoil section that the midplane of the airfoil (a plane parallel to the lower surface and distant from it by an amount equal to one-half the maximum thickness of the airfoil) contained the center of each block. The airfoils are designated in this report as Nos. 1 to 6, 1 being the thinnest, of 0.10 camber ratio and 6 the thickest of 0.20 camber ratio.

The balance used for the force measurements was designed by Dr. L. J. Briggs and built by Mr. W. H. Cottrell at the Bureau of Standards. Two views are shown in Figures 1 and 2, a few parts being removed in Figure 2 for clearness. A diagrammatic sketch is shown in Figure 3. The airfoil was held in a fork (A) in such a manner that it could be placed at any desired angle to the air stream. In addition it could be moved in the fork parallel to its chord so that any line in the midplane of the airfoil parallel to its leading edge and within an interval of 0.75 inch extending forward from the center of the airfoil could be placed in the axis of rotation. These adjustments were made possible by mounting on each arm of the fork a rotatable block (B) containing a groove in which the rectangular block (C) forming the end of the airfoil could slide. The airfoil was secured by square holding bolts (D) which passed through square holes in the airfoil and rectangular slots in the rotatable blocks. The axes of the two rotatable blocks were in the same line and at right angles to the air stream. Suitable locking devices were placed on each block to lock the airfoil at any desired angle.

The fork was pivoted at (E) with a linkage at (F) to an oil-filled sylvphon (G) placed at its outer end. The force exerted by the end of the fork against the sylvphon produced a pressure which was transmitted to a Bourdon pressure gauge and thus the moment of the air force about the axis of rotation of the fork was determined. When the air force passed through the axis of rotation of the airfoil this moment was produced by the drag component alone and the drag was readily computed. When the force did not intersect the axis, a suitable correction was applied for the moment of the lift component, from a knowledge of midplane center of pressure positions (points of intersection of air force with the midplane of the airfoil) inferred from the angle at which the moment of the air force was zero.

The pivot (E) of the fork was carried by an upright member (H) pivoted at its base (I). The lift force transmitted to this member was transmitted to a second upright member (K) by a strut and spring system (L). The second upright (K) was pivoted at its base (M) and carried a point (N) engaging a socket on a second sylvphon (O), the point and socket being in the plane of the axis of rotation of the airfoil and the axis of rotation of the fork about its pivot. The pressure in this sylvphon was transmitted to a second Bourdon gauge from whose readings the lift could be computed. The lift reading was independent of the position of the center of pressure.

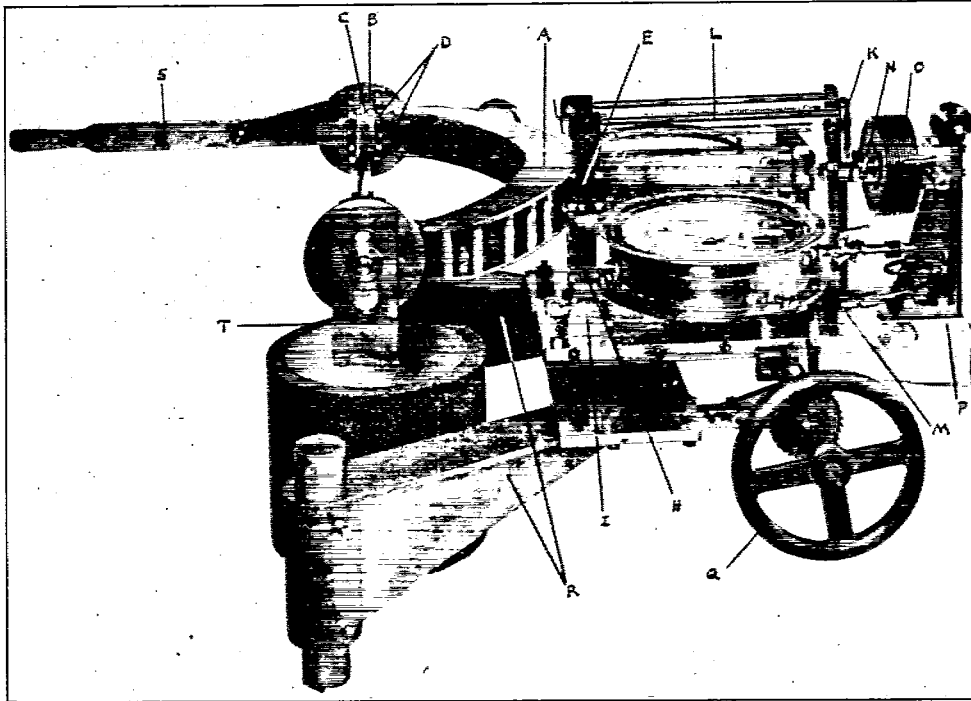


FIG. 1

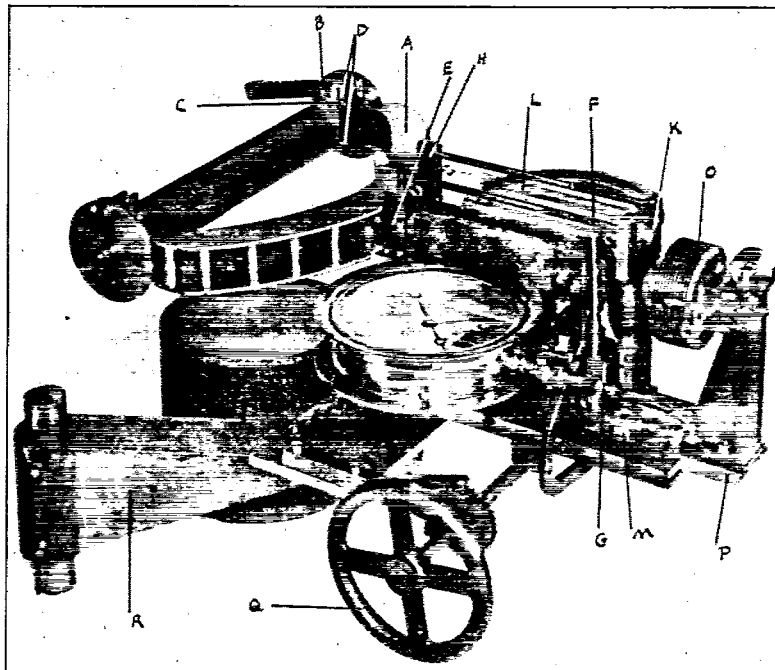


FIG. 2

Suitable counterweights were provided for producing initial pressure and for purposes of calibration. The whole balance including all parts heretofore described was mounted on a slide (P) on the underside of which was a rack engaging a pinion mounted on the base carrying the slide. By turning this pinion by means of a hand wheel (Q) the airfoil could be moved into or out of the stream at will. The base of the balance was carried on two brackets (R) which slid on vertical bars at each side of the orifice. The airfoil could therefore be placed at any distance from the mouth of the orifice and at any position relative to the center of the orifice.

A lever (S) was attached to one block and a balancing weight (T) to the other. The balancing weight could be adjusted so that with both blocks and the airfoil free to rotate about their common axis, the moment about that axis due to the weights of the various parts could be made zero for all angles of the airfoil. The angle of the airfoil to the wind for which the moment of the air force is zero could then be determined by unlocking the system and rotating the airfoil by means of the lever until there was no force exerted on the hand of the operator.

The speed of the air stream was computed from the pressure and temperature of the air in the pipe before expansion, on the assumption that the expansion through the orifice is isentropic,

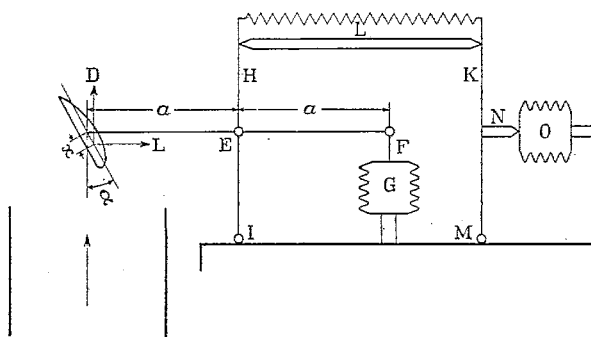


FIG. 3.—Diagrammatic sketch of balance

R_L = Reading on syphon O

R_D = Reading on syphon G

Lift = R_L

Drag = $R_D + (R_L \cos \alpha + R_D \sin \alpha) \frac{x}{a}$ approximately

that air is an ideal gas and that the pressure in the jet just outside the orifice is equal to the barometric pressure. Two gauges were used for measuring the excess pressure in the pipe. One, a mercury U-tube manometer, was connected to an impact tube in the pipe about 4 feet below the orifice. The other, a calibrated Bourdon gauge, was connected to a tube passing through the pipe wall and terminating flush with the inner surface about 4 feet below the orifice. The mercury manometer and impact tube formed the primary standard, but the Bourdon gauge and static plate calibrated in place were more convenient as a working standard. The readings of the

gauge connected to the impact tube included the additional pressure caused by the speed of approach of the air in the large pipe. The atmospheric pressure was determined by means of a standardized mercurial barometer.

The temperature of the air in the pipe was measured by means of four thermoelements distributed in a horizontal plane about 4 feet below the orifice mouth. Each element consisted of four copper Ideal junctions in series, the low temperature junctions being in an ice bath. The elements were calibrated at the Bureau of Standards. The electromotive force resulting from the temperature difference was measured by a Leeds and Northrup potentiometer and galvanometer.

The formula for the speed computed on the assumptions mentioned above is—

$$V^2 = 2 J C_p T_1 \left\{ 1 - \left(\frac{P_o}{P_i} \right)^{\frac{k-1}{k}} \right\} = 2 J C_p (T_1 - T_o)$$

where V = speed of air in cm. per sec.,

J = mechanical equivalent of heat,

C_p = specific heat of air at constant pressure,

k = ratio of specific heats,

T_1 = absolute temperature in pipe before expansion,

T_o = absolute temperature in jet after expansion,

P_i = impact pressure inside pipe,

P_o = pressure in jet (assumed equal to the barometric pressure).

RESULTS

The results of the force measurements are expressed in terms of the nondimensional or absolute coefficients used by aeronautical engineers and aerodynamical physicists. The principle of dimensional homogeneity indicates that the relationship between the force on a given body with respect to which air is moving is expressed by the relation

$$F = \frac{1}{2} \rho V^2 L^2 f \left(\frac{\rho V L}{\mu}, \frac{V}{c} \right)$$

where F is the force, ρ the air density, V the air speed, L the linear dimension determining the scale, μ the viscosity of the air, and c the speed of sound. At the high speeds involved in the present work the influence of viscosity is generally supposed to be negligible. With this assumption the laws for the lift component normal to the wind direction and the drag component parallel to the wind direction may be expressed as follows:

$$C_L = \frac{\text{Lift}}{\frac{1}{2} \rho V^2 \text{Area}} = \phi \left(\frac{V}{c} \right)$$

$$C_D = \frac{\text{Drag}}{\frac{1}{2} \rho V^2 \text{Area}} = \phi_1 \left(\frac{V}{c} \right)$$

C_L and C_D are plotted against $\frac{V}{c}$, c being computed for the temperature of the air in the jet, the value at 0° C. being assumed to be 1,088 ft./sec. The area of the airfoil to be used is uncertain because of the unknown end effects. The length of the airfoil was taken equal to the diameter of the mouth of the orifice.

Expression of the results in this form has many advantages. In the first place, a broader interpretation of the results is possible, the number of independent variables having been reduced from five to two. In the second place, the values do not depend on the system of units employed. In the third place, the deviations from the usually assumed square law are readily apparent, since a square law is indicated by a constant coefficient. From the character of the coefficient curves it is apparent that any one of the airfoils at an angle of say 8° to the wind is aerodynamically an entirely different body from the same airfoil at -4°, the manner in which the force varies with the speed being quite different in the two cases.

The coefficients computed from the individual observations are given without fairing of any kind in plots of the coefficients against V/c . (See figs. 4 to 9 and 16 to 21, inclusive.) Faired values of the coefficients for given values of V/c are replotted against the angle of the airfoil to the wind (measured from the plane of the flat lower surface) to give the familiar lift and drag curves of the type usually plotted for airfoils. (Figs. 10-15, and 22-27.) In the original fairing no attempt has been made to make the curves belong to families, the observed points being closely followed.

Considering first the variation of C_L with V/c (figs. 4-9) we find in the case of the thickest airfoil (fig. 9) the coefficient is sensibly constant for angles close to 0° for values of V/c less than 0.65; it increases with speed as greater negative angles are reached; and it decreases with speed as greater positive angles are reached. In the case of the thinner airfoils, the lift coefficient at low angles of attack does not change sensibly until higher values of V/c are reached. For values of V/c greater than this critical value (if we may so term it, although it is not sharply defined) the lift coefficient decreases with speed very rapidly for all angles. Even in the case of the negative angles, although the course of the rapid decrease is shown only in the case of airfoil 3 (fig. 6), the decrease is known to occur; for the values at the higher speeds were negative and could not be measured, since the balance was designed for positive lifts only.

When the faired values of C_L are plotted against angle of attack α (figs. 10-15) for selected values of V/c these same characteristics are shown in another way. We shall choose airfoil 3 (fig. 12) as a typical example, the effects being less pronounced for the thinner airfoils and more pronounced for the thicker airfoils. The curves for the several values of V/c less than 0.8 cross in the neighborhood of -2°. For angles greater than this the curves for higher speeds lie lower

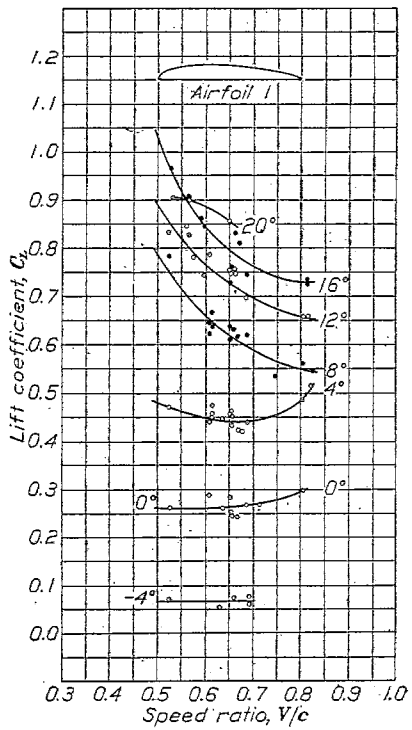


FIG. 4

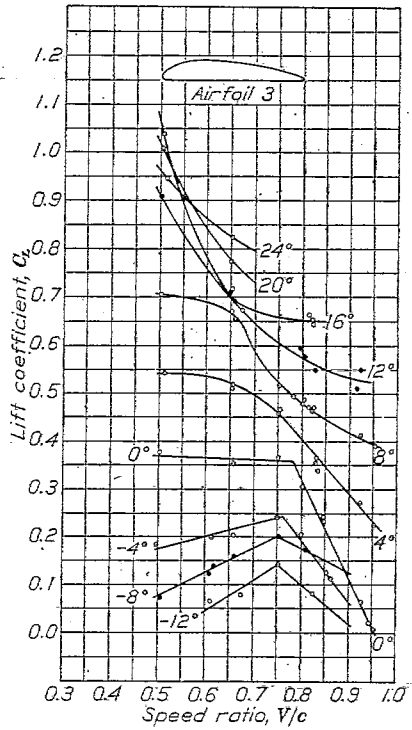


FIG. 6

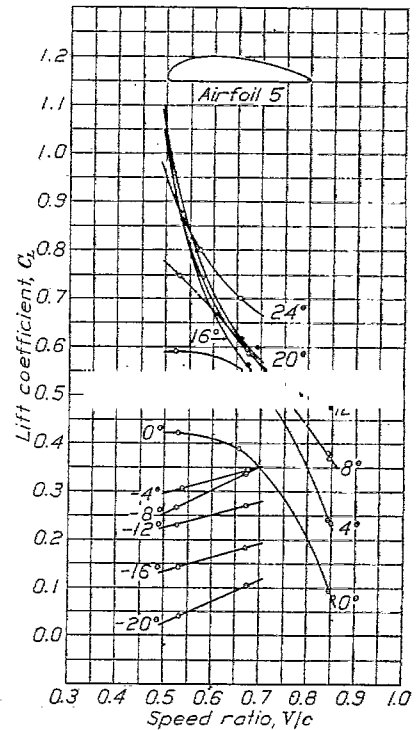


FIG. 8

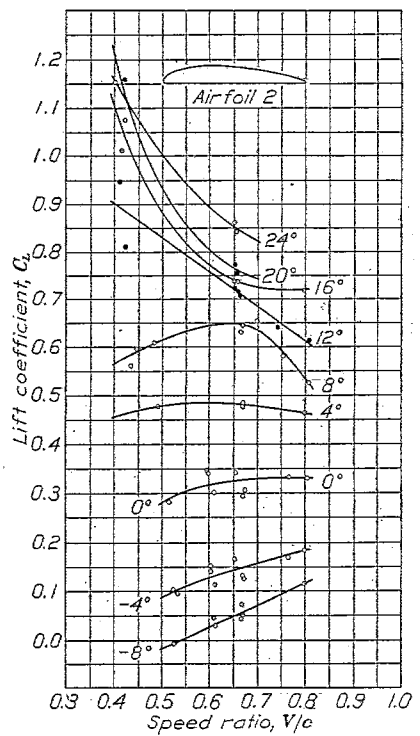


FIG. 5

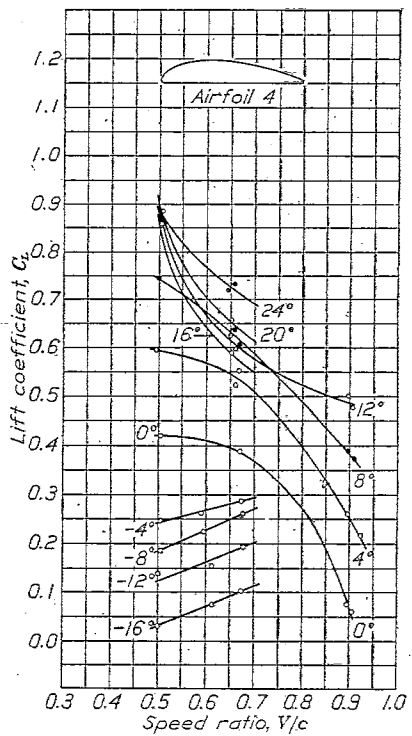


FIG. 7

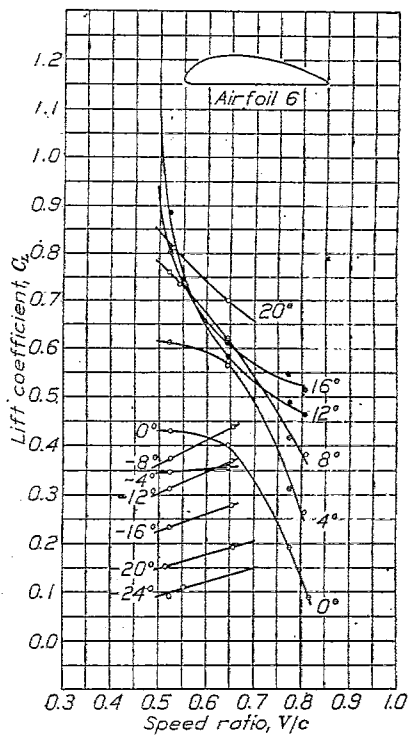


FIG. 9

Lift coefficient, C_L vs. V/c . Various values of α

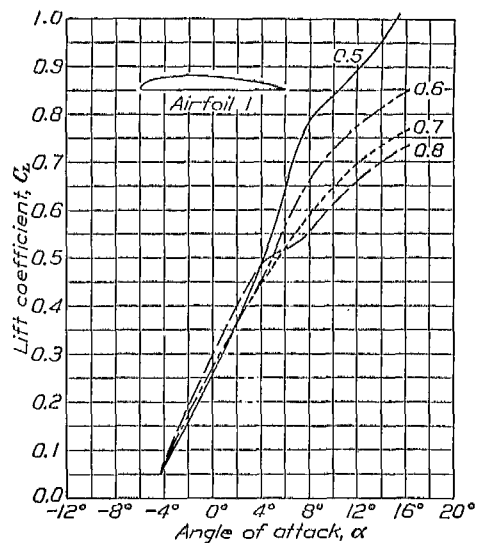


FIG. 10

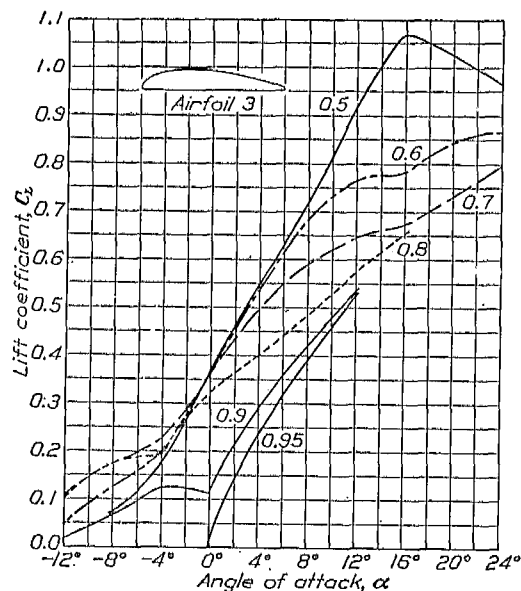


FIG. 12

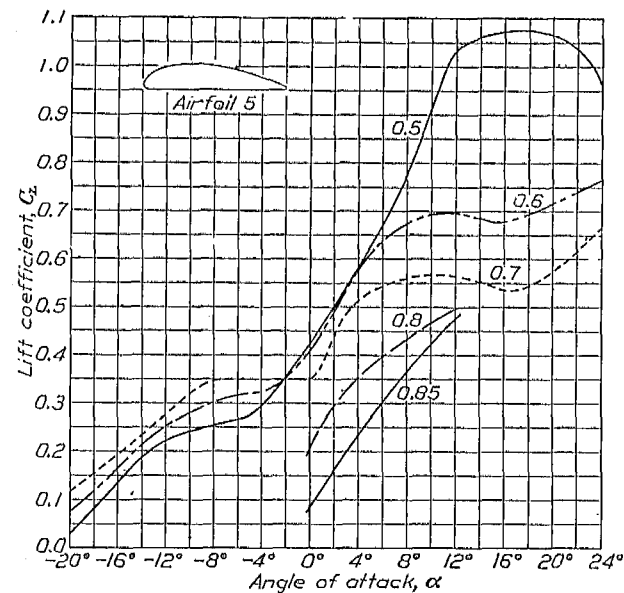


FIG. 14

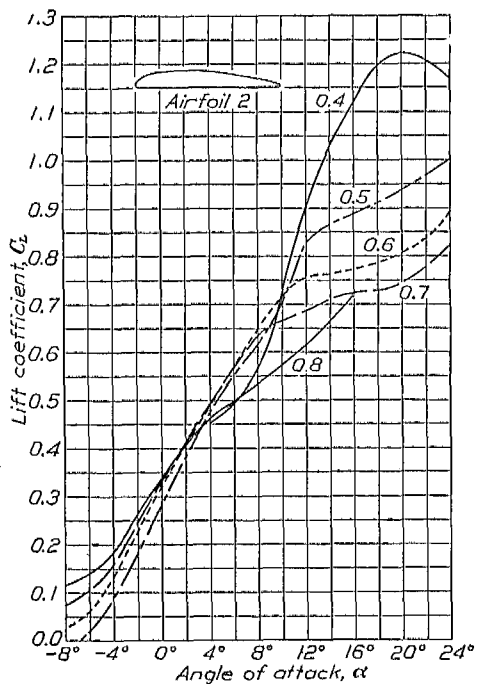


FIG. 11

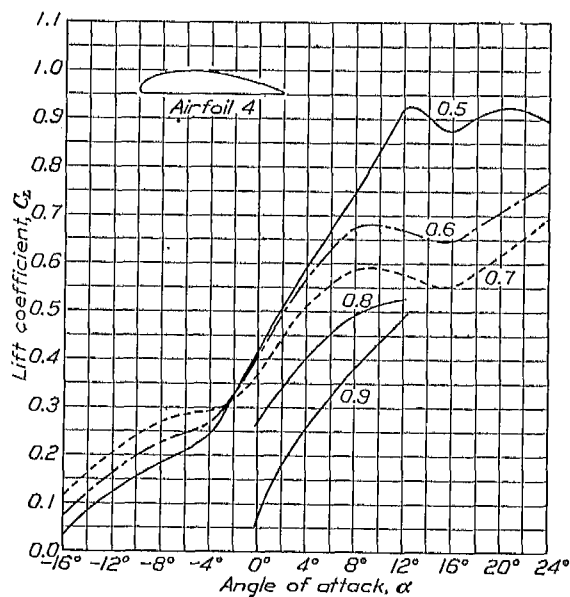


FIG. 13

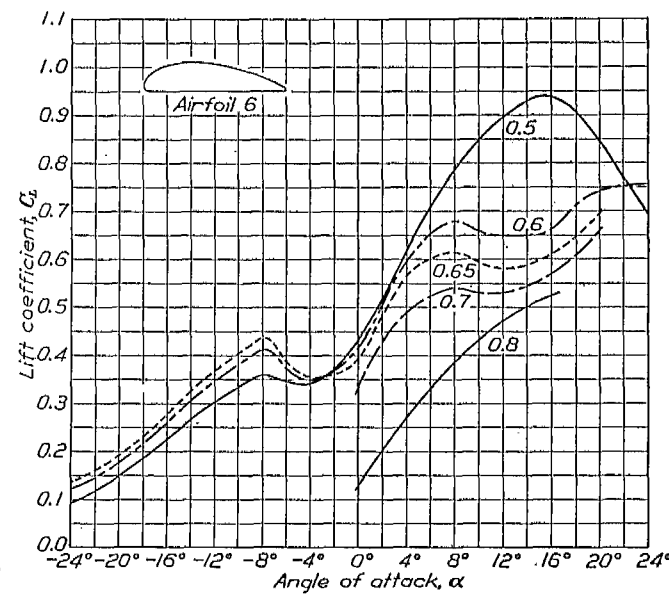


FIG. 15

Lift coefficient, C_L vs. α . Various values of V/c

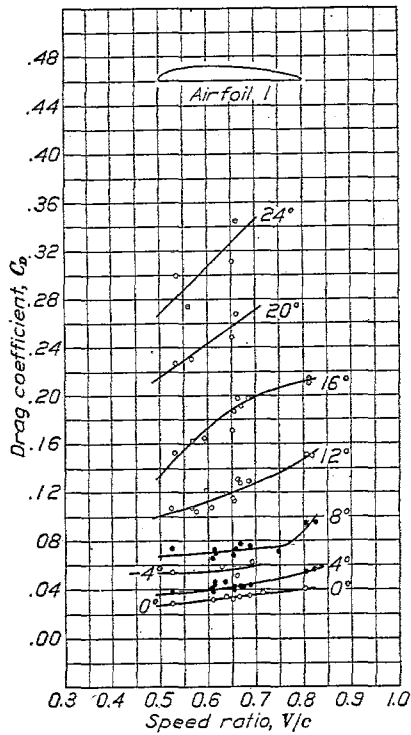


FIG. 16

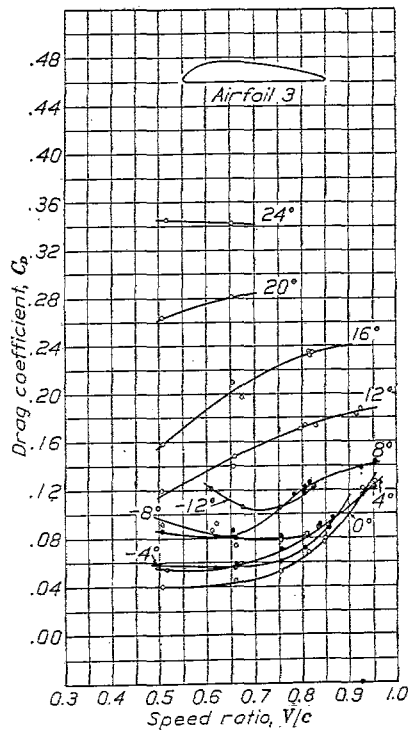


FIG. 18

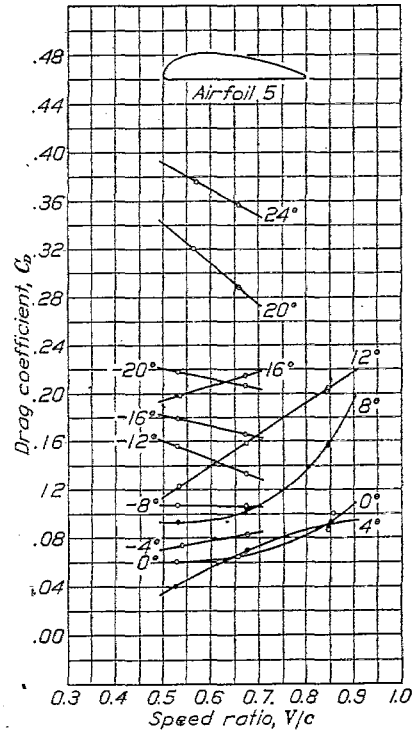


FIG. 20

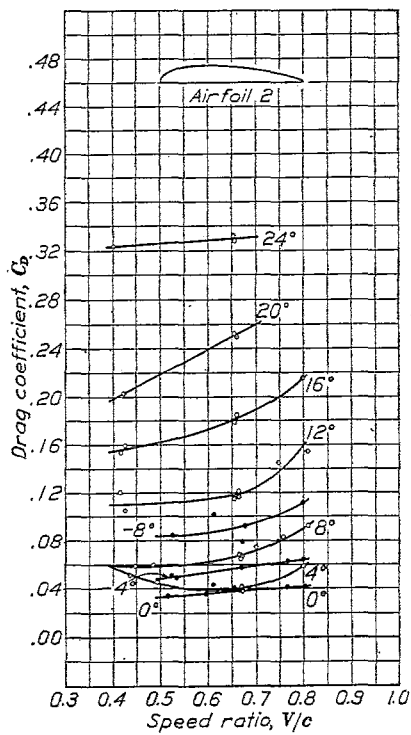


FIG. 17

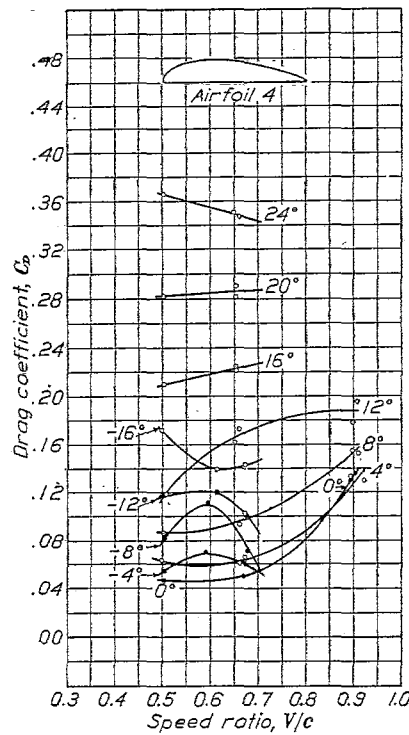


FIG. 19

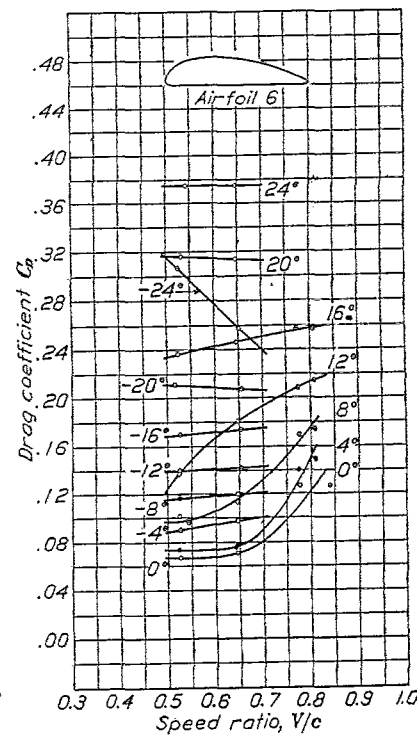


FIG. 21

Drag coefficient, C_D vs. V/c . Various values of α

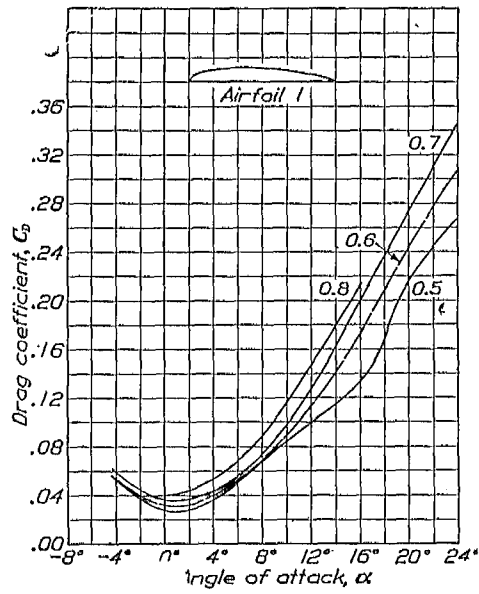


FIG. 22

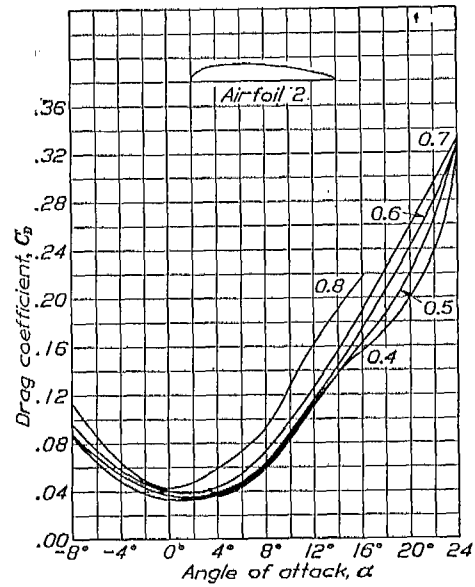


FIG. 23

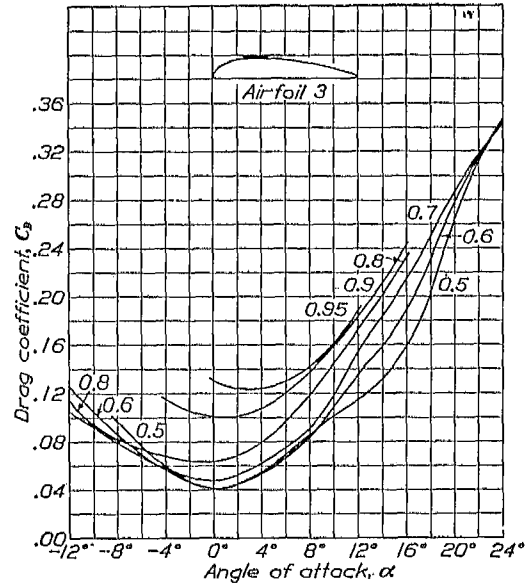


FIG. 24

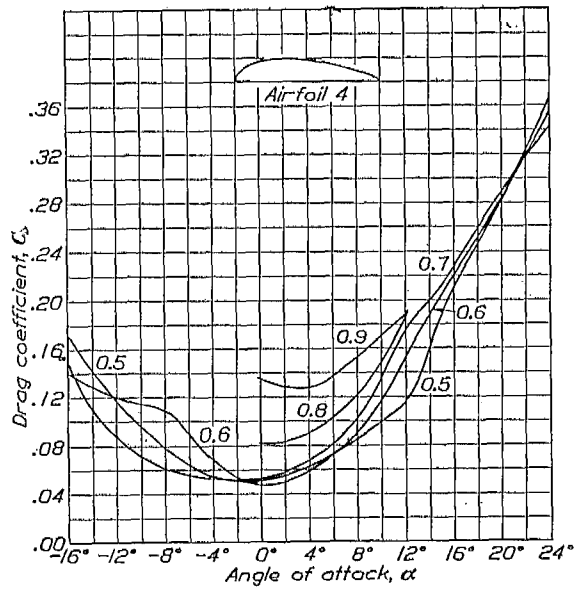


FIG. 25

Drag coefficient, C_D vs. α . Various values of V/c

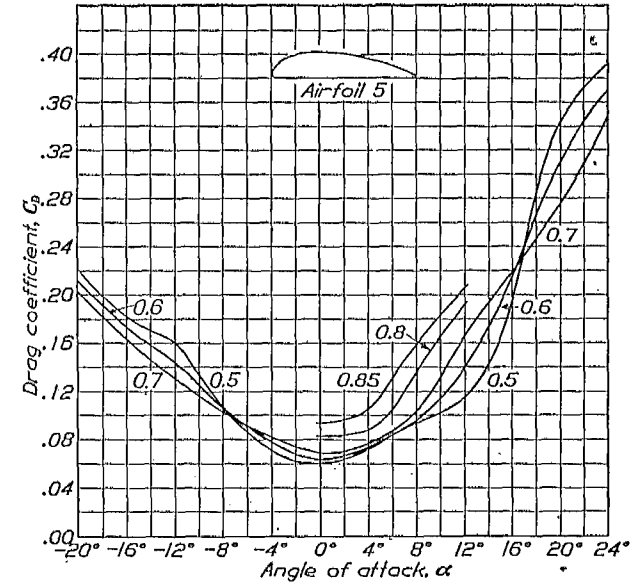


FIG. 26

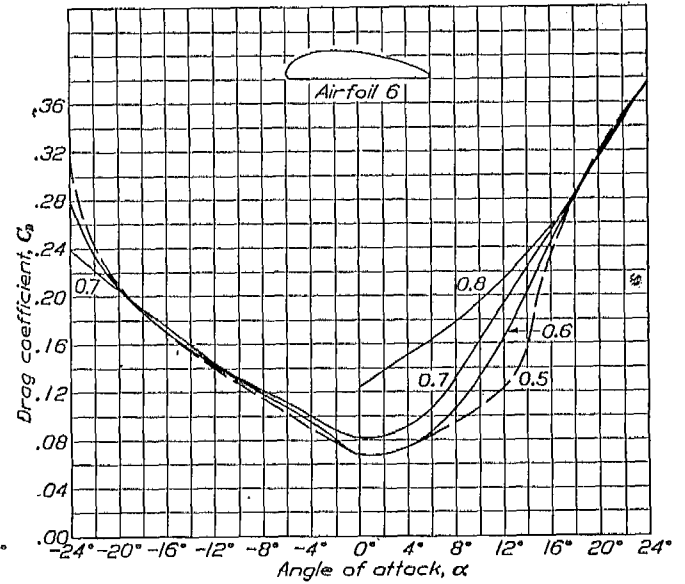


FIG. 27

in the diagram; for smaller angles the curves for higher speeds lie higher. The angle of no lift shifts with increasing speed toward greater negative angles. For values of V/c greater than 0.8 the general behavior at high angles remains unchanged, the curves for the higher speeds being the lower. The behavior at negative angles is reversed, the curves for higher speeds no longer being higher but very much lower and the angle of no lift shifts rapidly toward 0° with increasing speeds.

In the case of airfoils 5 and 6 (figs. 14, 15) subsidiary maxima occur in the C_L versus α curves as in the case of measurements in wind tunnels at much lower speeds.

Turning now to the curves of C_D versus V/c (figs. 16-21) we find conditions somewhat different. In general C_D increases with V/c . For high angles there is an approach to constancy while for negative angles of the thicker airfoils (figs. 19-21) there are instances of a decrease with speed. As has been explained the computation of the drag depends on a knowledge of the position of the midplane center of pressure because of the design of the balance. The midplane center of pressure at negative angles could not be measured and estimated values were used. For this reason the values at negative angles are not as accurate as those at positive angles but we do not believe that the general behavior is materially different from that shown. For the thicker airfoils at high values of V/c (figs. 19-21) at moderate angles the rate of increase of C_D is much accelerated. The value of V/c at which this rate of increase changes materially corresponds roughly to the "critical values" for the lift. The "critical value" is a function of the angle of the airfoil to the wind as well as of the thickness of the airfoil. Beyond 8° or 12° the rate of increase is not so great, a fact that will be referred to later.

The curves of C_D versus α for selected values of V/c (figs. 22-27) are not essentially different from those obtaining at ordinary wind-tunnel speeds. The crossing at negative angles is first shown in the case of airfoil 3 (fig. 24).

The results are plotted in a form more suitable for theoretical interpretation in Figures 28-33. C_L is plotted against C_D giving the polar diagram.³ A part of the drag is due to the finite size of the stream and to the fact that it is not confined. In producing a given lift, transverse momentum is imparted to the stream and the jet is deflected. The deflection begins ahead of the airfoil and changes the angle of attack of the air on the airfoil. Neglecting the change in the shape of the jet and any influence due to the proximity of the orifice within which no deflection can occur, the drag induced by the change in angle may be computed.⁴ The induced drag is the same as for an airfoil of length equal to the jet diameter in an infinite stream, namely

$$\frac{C_L^2}{\pi \times \text{aspect ratio}}$$
 The induced drag curve is plotted on each of the polar diagrams.

The difference between the total drag and the induced drag, which is termed the profile drag, is not constant even at the lower speeds. At lift coefficients below about 0.4, which occur at negative angles of attack, the profile drag is very complex. At high speeds the profile drag increases more and more for a given lift coefficient and lower maximum lifts are obtained.

The observations of angle of no torque used in estimating midplane center of pressure positions are shown as plots of angle of attack for zero torque versus V/c for various positions of the torque axis (figs. 34-39). The position of the torque axis gives the center of pressure position referred to the midplane of the airfoil at the angle of attack giving no torque. This position is measured from the nose and is expressed as a fraction of the chord. The values for airfoils 3 and 5 (figs. 36-38) best illustrate the form of the curves. At high speeds a point is reached where the midplane center of pressure never reaches the torque axis for any angle of attack. This is shown by direct observation and indicates that the curves go off asymptotic to vertical lines. The observations are not sufficiently numerous to enable well-defined center of pressure curves to be plotted, but they indicate that the midplane center of pressure at any given angle moves rapidly back as the speed is increased, and more rapidly at the higher speeds. The effects again are more pronounced for the thicker airfoils, beginning at lower speeds. That the center of

³ In this second cross plot of the data it has been found advisable in a few cases to make some additional fairing.

⁴ For a detailed derivation and some discussion as to the validity of the assumptions, see H. Kumbusch, *Zeitschrift für Flugtechnik und Motorluftschiffahrt*, vol. 10, Nos. 9 and 10.

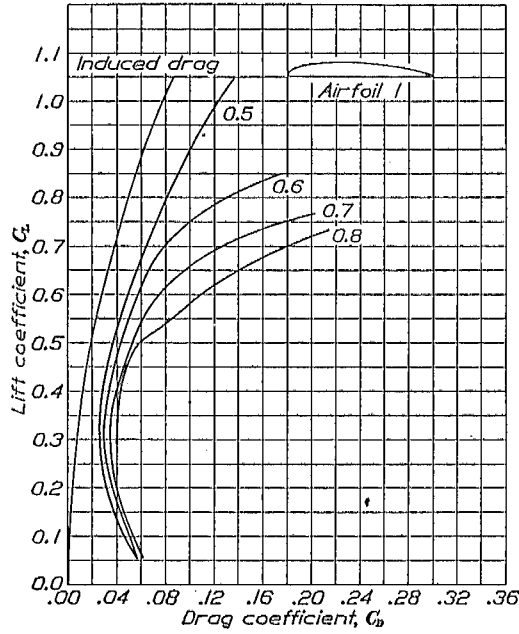


FIG. 28

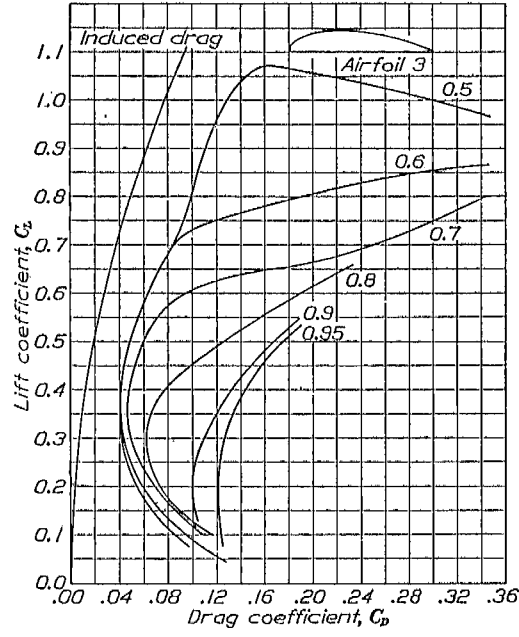


FIG. 30

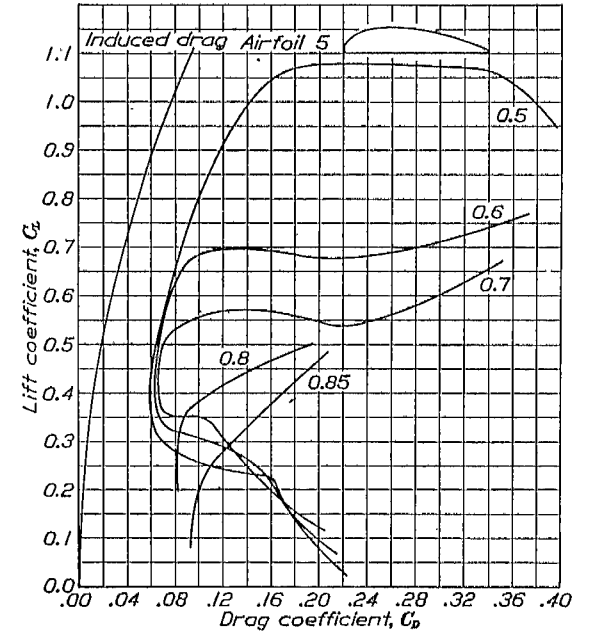


FIG. 32

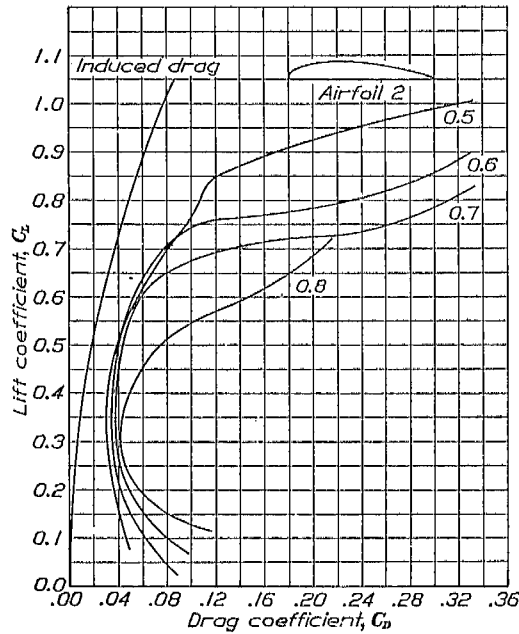


FIG. 29

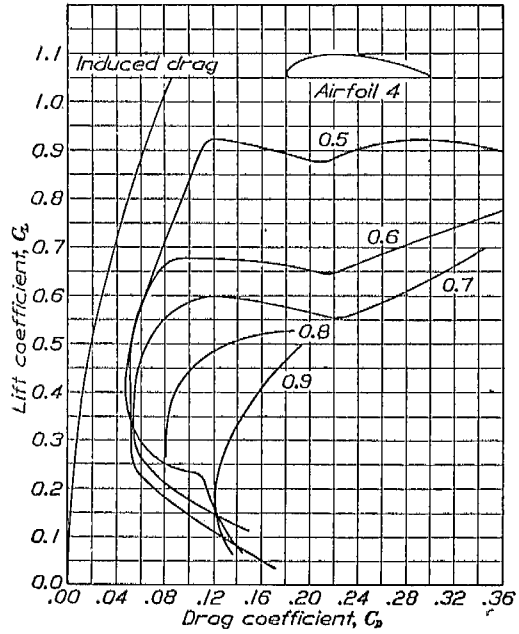


FIG. 31

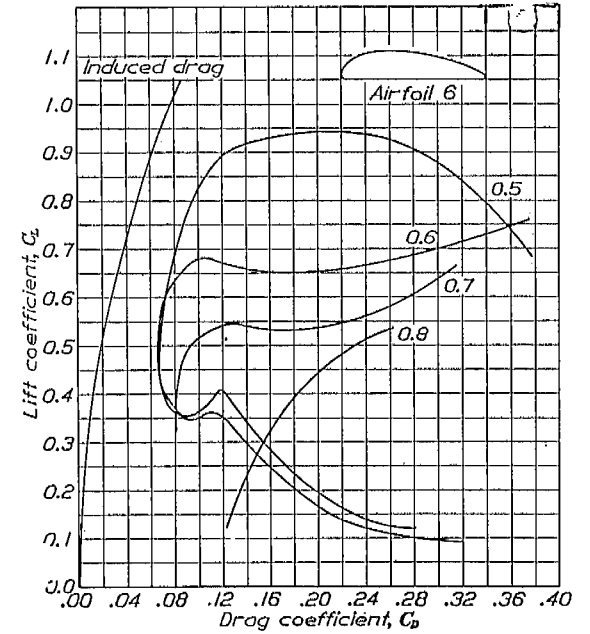


FIG. 33

Polar diagrams, C_L vs. C_D . Various values of V/c

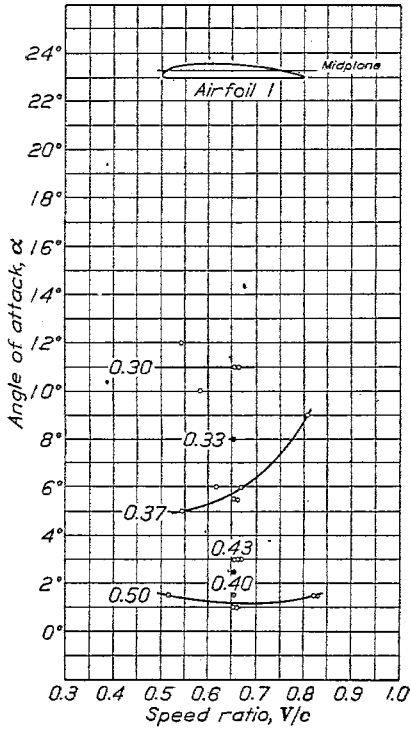


FIG. 34

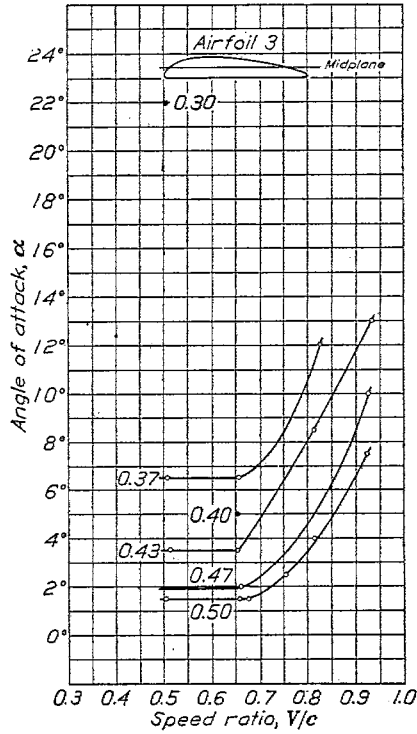


FIG. 36

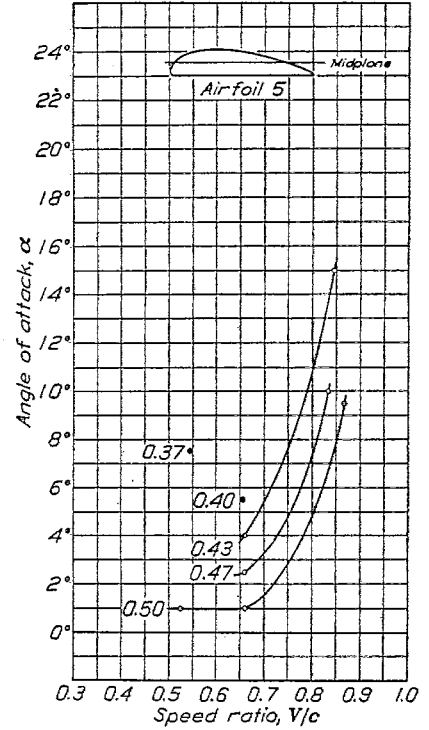


FIG. 38

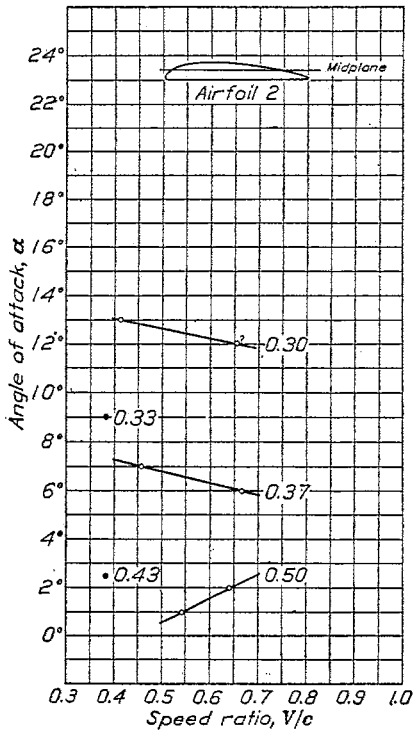


FIG. 35

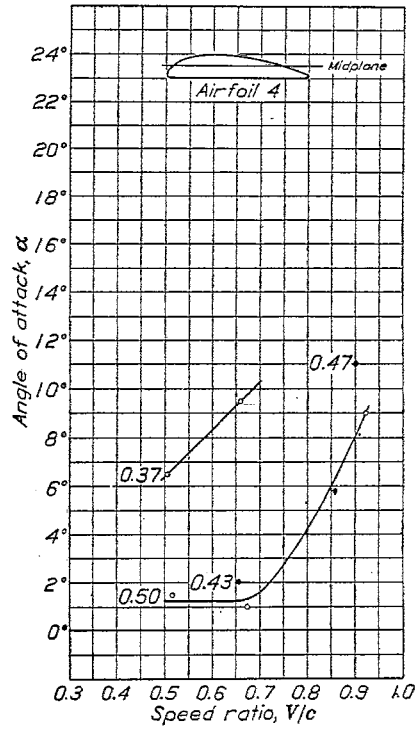


FIG. 37

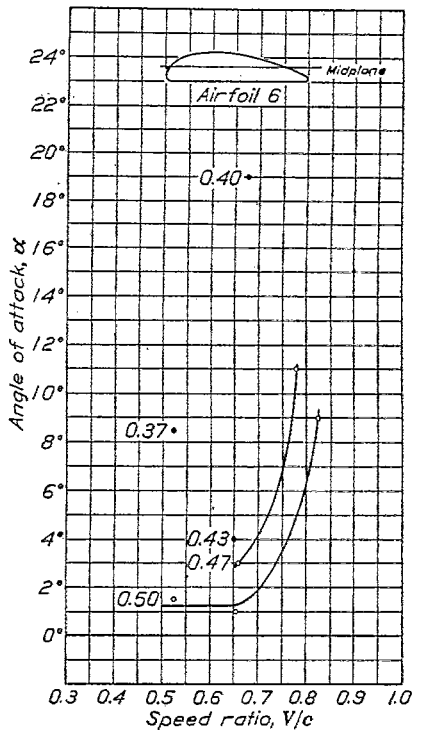


FIG. 39

No torque angle of attack, α vs. V/c . Various positions of midplane center of pressure expressed as a fraction of chord

pressure referred to the chord also moves back is shown by the vector diagrams for airfoil 3 in Figure 40.

Attention has been called to the change in behavior of the drag versus V/c curves from 8° to 12° . During some of the tests in bad weather oil was placed on the airfoils to keep them from rusting. On entering the stream most of the oil was blown off the surface but some remained on the rounded trailing edge. As the angle of attack reached about 8° this column of oil along the trailing edge began to flow down on the upper surface near the center, winding in two symmetrical spirals. The flow was toward the leading edge at the center of the span, then out toward the tips and in toward the trailing edge. This indicates the formation of a vortex pair and a consequent change in flow. Since the vortices form symmetrically with respect to the center of the jet, the change in flow is probably associated in some way with the end effects. Only a few observations of this character were made so that no close correlation of vortex formation and force curves can be made.

The meaning of all these changes is not entirely clear. The most reasonable hypothesis as to what is going on and one which fits in fairly well with general considerations is as follows. We may suppose that the speed of sound represents an upper limit beyond which an additional loss of energy takes place. If at any place on the wing then the velocity of sound is reached, the drag will increase. From our knowledge of the flow around airfoils at ordinary speeds we know that the velocity near the surface of the airfoil is much higher than the general stream velocity. The increase depends on the angle and on the form of section, usually being greater for the larger angles and thicker sections. This corresponds very well with the earlier breakdown of the thicker wings and of all the wings at high angles.

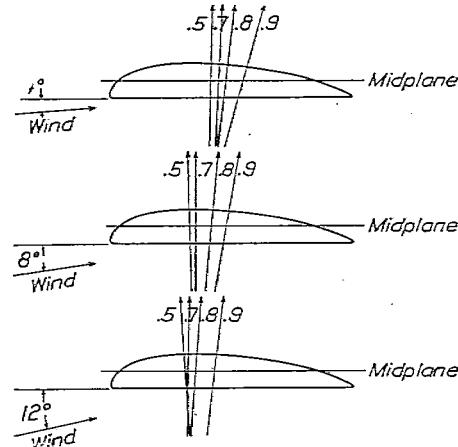


FIG. 40.—Vector diagrams for airfoil 3, travel of $C. P.$ with V/c at various values of α

NOTE.—Vectors show direction not magnitude

PRECISION OF RESULTS

The large power consumption of the compressor (5,000 horsepower at high speeds) and the high cost of operation have made it impossible to repeat observations at will. In the interest of economy, many of the measurements were made while the compressors were being put through commercial shop tests. During such tests, the speed of the air stream was not under our control, and the speed would often vary before a complete set of observations could be made. The noise of the air stream was so great that it was difficult for the observers to communicate with each other while the compressor was running so that modification of the program to meet changing conditions was difficult.

The character of the flow about the model spanning the air stream differs materially from the conditions of flow either around an infinitely long airfoil or around an airfoil of finite span. It is supposed that for angles less than 8° at least the conditions approximate most nearly to those around an airfoil of infinite length, in other words that the flow around the airfoil is approximately two-dimensional in character.

The distribution of speed across the jet was very nearly constant except near the edge of the jet. Tests on the thinnest airfoil showed no differences in the measured force over a range from 4 inches above the orifice mouth to 15 inches above the mouth.

The alignment of the balance with the air stream was checked by reversing the airfoil. Measurement could only be made in the region close to zero lift but no systematic differences were found.

Errors arising from imperfections of the balance may combine to cause uncertainties of the order of ± 2 per cent. In the case of the drag at negative angles of attack the midplane

center of pressure position is not known so that the values given are in the nature of estimates. The error, however, is not likely to be greater than 5 per cent. In general, we may say that the actual forces on the airfoils as mounted in the jet are known to about 2 per cent; but the application of the results to numerical calculations for infinite airfoils or airfoils of any aspect ratio in a uniform and infinite stream is subject to greater and unknown errors.

COMPARISON WITH PREVIOUS WORK

The airfoils tested in the 14-inch high-speed wind tunnel at McCook Field, mentioned earlier in the paper, were of the same form as those used in this work. The airfoils were of 1 inch chord and 6 inch span, supported by a spindle about $\frac{3}{4}$ inch in diameter extending forward from the leading edge to the balance outside the mouth of the tunnel. Speeds just overlapping the region here investigated were reached. Attempts at numerical correlation of the data have proven unsuccessful but this is not surprising in view of the different scale of the models, the different methods of support, and the different end conditions. The qualitative results agree remarkably well. The shift of the angle of no lift to greater negative angles, the greater effects of change in speed on the thicker wings and the flatness of the C_L versus α curves at negative angles were observed at McCook Field. The crossing of the C_L versus α curves was also noted. No drag measurements or center of pressure measurements were obtained and the limitation of speed prevented the attaining of the critical point for small angles. A vortex formation was observed which while nearer the wing tips was in general similar to that described here.

The agreement of the results here presented with tests on an actual propeller may be seen by comparison with the conclusions reached in R. & M. No. 884. The thrust was deduced from flight tests of a high tip speed propeller, and measurements were made of thrust, torque, thrust grading, and blade angles under running conditions on a model in a wind tunnel. The conclusions reached in the British report were as follows:

1. Higher tip speeds than at present used will probably involve a serious loss in efficiency.
2. Lift coefficients increase considerably above 0.6 the speed of sound, reaching a maximum at about 0.8 after which they probably decrease. Center of pressure travels back at high speeds and drag coefficients increase.

The statement as to lift coefficient applied to a section at the tip of camber ratio 0.10 corresponding to air foil No. 1 of the present series. The increase in lift computed from the increase in thrust is somewhat larger than that observed for airfoil No. 1.

CONCLUSIONS

The experiments show that at high speeds the important aerodynamic characteristics of airfoils of the form commonly used as propeller sections are as follows:

1. The lift coefficient for a fixed angle of attack decreases very rapidly as the speed increases.
2. The drag coefficient increases rapidly.
3. The center of pressure moves back toward the trailing edge.
4. The speed at which the rapid change in the coefficients begins is decreased by (a) increasing the angle of attack and by (b) increasing the camber ratio.
5. The angle of zero lift shifts to high negative angles up to the "critical speed" and then moves rapidly toward 0° .

In terms of the characteristics of propellers, these statements become:

1. The thrust coefficient for a given value of V/ND decreases at high speeds.
2. The power coefficient increases.
3. The twisting moment of the blade becomes less.
4. The rapid changes in the thrust and power coefficients begin at lower tip speeds for propellers of thick section than for propellers of thin section. For a given propeller the change occurs earlier at low values of V/ND than at high values.
5. The experimental mean pitch or virtual pitch increases to a maximum and then decreases.

It must be remembered that even when the tip speed equals the speed of sound only the tip section travels at this speed, all others being at lower speeds and that usually the tip section is thin. The numerical magnitude of the changes to be expected for any given propeller may be computed from the data given in this paper.

TABLE 1
DIMENSIONS OF AIRFOILS

Airfoil No. 1			Airfoil No. 3			Airfoil No. 5		
	Nominal value	Measured value		Nominal value	Measured value		Nominal value	Measured value
Length.....	Inches 17.200	Inches 17.202-17.205	Length.....	Inches 17.200	Inches 17.203-17.204	Length.....	Inches 17.200	Inches 17.190-17.192
Chord.....	3.000	2.998- 2.999	Chord.....	3.000	2.995	Chord.....	3.000	2.997- 2.998
Distance of station aft of leading edge	Ordinate at station		Distance of station aft of leading edge	Ordinate at station		Distance of station aft of leading edge	Ordinate at station	
	Nominal value	Measured value		Nominal value	Measured value		Nominal value	Measured value
Inches	Inch	Inches	Inches	Inch	Inches	Inches	Inch	Inches
0.075	0.123	0.123-0.124	0.075	0.171	0.170-0.171	0.075	0.219	0.220-0.221
.150	.177	.177	.150	.246	.245-.245	.150	.318	.316-.317
.300	.237	.235-.238	.300	.330	.328-.331	.300	.426	.428-.429
.600	.285	.284-.288	.600	.399	.397-.400	.600	.513	.510-.512
.900	.300	.298-.303	.900	.420	.415-.420	.900	.540	.535-.537
1.200	.297	.297-.302	1.200	.414	.412-.416	1.200	.534	.532-.534
1.500	.285	.286-.290	1.500	.399	.395-.399	1.500	.513	.510-.511
1.800	.261	.262-.271	1.800	.363	.361-.364	1.800	.468	.465-.466
2.100	.222	.223-.227	2.100	.309	.306-.309	2.100	.399	.395-.396
2.400	.168	.171-.174	2.400	.234	.235-.237	2.400	.300	.298-.300
2.700	.105	.108-.111	2.700	.147	.147-.149	2.700	.189	.185-.186
Airfoil No. 2			Airfoil No. 4			Airfoil No. 6		
	Nominal value	Measured value		Nominal value	Measured value		Nominal value	Measured value
Length.....	Inches 17.200	Inches 17.205-17.207	Length.....	Inches 17.200	Inches 17.190-17.193	Length.....	Inches 17.200	Inches 17.205-17.207
Chord.....	3.000	2.999- 3.000	Chord.....	3.000	3.000	Chord.....	3.000	2.999
Distance of station aft of leading edge	Ordinate at station		Distance of station aft of leading edge	Ordinate at station		Distance of station aft of leading edge	Ordinate at station	
	Nominal value	Measured value		Nominal value	Measured value		Nominal value	Measured value
Inches	Inch	Inches	Inches	Inch	Inches	Inches	Inch	Inches
0.075	0.147	0.146	0.075	0.195	0.195-0.196	0.075	0.246	0.246-0.247
.150	.210	0.208-.209	.150	.282	.280-.281	.150	.354	.351-.352
.300	.282	.282-.284	.300	.378	.380-.381	.300	.474	.475-.477
.600	.342	.340-.342	.600	.456	.458-.458	.600	.570	.570-.572
.900	.360	.359-.362	.900	.480	.480-.482	.900	.600	.600-.602
1.200	.354	.354-.357	1.200	.474	.474-.477	1.200	.594	.592-.596
1.500	.342	.341-.343	1.500	.456	.455-.457	1.500	.570	.568-.572
1.800	.312	.312-.314	1.800	.417	.416-.419	1.800	.522	.519-.524
2.100	.264	.266-.268	2.100	.354	.354-.357	2.100	.444	.437-.441
2.400	.201	.203-.206	2.400	.267	.269-.272	2.400	.336	.333-.337
2.700	.126	.129-.131	2.700	.168	.167-.171	2.700	.210	.211-.215

NOTE.—The values for the first two ordinates are direct measurements between two points. For the other ordinates the airfoil was placed on a surface plate and indicated. Such values may be somewhat high since the airfoil rests on high points of the flat lower surface. In the case of airfoils 1, 2, 4, and 6 the values within a few inches of one end were higher than the remaining portion.